

Diffusion Kurtosis Imaging Detects Microstructural Alterations in Brain of α -Synuclein Overexpressing Transgenic Mouse Model of Parkinson's Disease: A Pilot Study

Amit Khairnar¹ · Peter Latta² · Eva Drazanova^{3,5} · Jana Ruda-Kucerova^{4,5} ·
Nikoletta Szabó⁶ · Anas Arab^{4,5} · Birgit Hutter-Paier⁷ · Daniel Havas⁷ ·
Manfred Windisch⁸ · Alexandra Sulcova⁴ · Zenon Starcuk Jr.^{3,2} · Irena Rektorova¹

Received: 24 October 2014 / Accepted: 29 June 2015 / Published online: 8 July 2015
© Springer Science+Business Media New York 2015

Abstract Evidence suggests that accumulation and aggregation of α -synuclein contribute to the pathogenesis of Parkinson's disease (PD). The aim of this study was to evaluate whether diffusion kurtosis imaging (DKI) will provide a sensitive tool for differentiating between α -synuclein-overexpressing transgenic mouse model of PD (TNWT-61) and wild-type (WT) littermates. This experiment was designed as a proof-of-concept study and forms a part of a complex protocol and ongoing translational research. Nine-month-old TNWT-61 mice and age-matched WT littermates underwent behavioral tests to monitor motor impairment and MRI scanning using 9.4 Tesla system in vivo. Tract-based spatial statistics (TBSS) and the DKI protocol were used to compare the whole brain white matter of TNWT-61 and WT mice. In addition, region of interest (ROI) analysis was performed in gray matter regions such as substantia nigra, striatum, hippocampus, sensorimotor cortex, and thalamus known to show higher

accumulation of α -synuclein. For the ROI analysis, both DKI (6 *b*-values) protocol and conventional (2 *b*-values) diffusion tensor imaging (cDTI) protocol were used. TNWT-61 mice showed significant impairment of motor coordination. With the DKI protocol, mean, axial, and radial kurtosis were found to be significantly elevated, whereas mean and radial diffusivity were decreased in the TNWT-61 group compared to that in the WT controls with both TBSS and ROI analysis. With the cDTI protocol, the ROI analysis showed decrease in all diffusivity parameters in TNWT-61 mice. The current study provides evidence that DKI by providing both kurtosis and diffusivity parameters gives unique information that is complementary to cDTI for in vivo detection of pathological changes that underlie PD-like symptomatology in TNWT-61 mouse model of PD. This result is a crucial step in search for a candidate diagnostic biomarker with translational potential and relevance for human studies.

Electronic supplementary material The online version of this article (doi:10.1007/s12640-015-9537-9) contains supplementary material, which is available to authorized users.

✉ Irena Rektorova
irena.rektorova@ceitec.muni.cz

- ¹ Applied Neuroscience Research Group, CEITEC - Central European Institute of Technology, Masaryk University, Kamenice 5, 625 00 Brno, Czech Republic
- ² Multimodal and Functional Imaging Laboratory, CEITEC - Central European Institute of Technology, Masaryk University, Brno, Czech Republic
- ³ Institute of Scientific Instruments, Academy of Sciences of the Czech Republic, Brno, Czech Republic
- ⁴ Experimental and Applied Neuropsychopharmacology Group, CEITEC - Central European Institute of Technology, Masaryk University, Brno, Czech Republic

Keywords Diffusion kurtosis imaging · α -Synuclein · TNWT-61 · Parkinson's disease · Transgenic mice · TBSS

- ⁵ Department of Pharmacology, Faculty of Medicine, Masaryk University, Brno, Czech Republic
- ⁶ Department of Neurology, Faculty of Medicine, Albert Szent-Györgyi Clinical Centre, University of Szeged, Szeged, Hungary
- ⁷ QPS Austria GmbH, Grambach, Austria
- ⁸ NeuroScios GmbH, Graz, Austria

Introduction

Treatment options for Parkinson's disease (PD) are limited to drugs elevating the brain dopamine levels by various mechanisms. However, this approach does not stop the neurodegenerative process. The development of “neuro-protective” treatments is a central challenge for future PD therapy. To evaluate efficacy and to monitor disease-modifying effects, reliable surrogate markers for early PD diagnosis and progression are needed when patients might still be eligible for neuroprotective treatment (Rascol et al. 2011; Stocchi and Olanow 2013).

Magnetic resonance imaging (MRI) in contrast to PET and SPECT relies on intrinsic tissue contrast generation and thus it is free from ionizing radiation, cheaper, and widely available. While standard protocols such as T1/T2 imaging have failed to detect the volume changes in the substantia nigra (SN) in early PD, recent advances in MRI, such as diffusion-weighted imaging (DWI) and namely diffusion tensor imaging (DTI), allow non-invasive in vivo assessment of tissue microstructure by mapping water proton motion within the tissue microenvironment (Lang and Mikulis 2009; Meijer and Goraj 2014). This is expressed in terms of two main variables: diffusivity, which is a measure for nature of water diffusion, and fractional anisotropy (FA), which is a measure of the directionality of diffusion (Boska et al. 2007; Lerner et al. 2013).

Several clinical and pre-clinical studies in PD have reported that diffusivity is increased and/or FA is reduced in the SN (Boska et al. 2007; Lang and Mikulis 2009; Soria et al. 2011; Cochrane and Ebmeier 2013; Vaillancourt et al. 2009). One recent DTI study has demonstrated a decrease in FA also in the anterior olfactory system at an early stage of PD (Rolheiser et al. 2011). Of note, two meta-analyses on DTI in PD patients have been published, one claiming that DTI is promising biomarker in Parkinsonian syndromes (Cochrane and Ebmeier 2013) while the other was actually questioning stability and validity of nigral FA changes (Schwarz et al. 2013). Taken together, the results of conventional DTI (cDTI) that uses only 2 *b*-values for data analysis have been controversial so far. Some authors recommend further studies with standardizing the anatomical position of SN to improve the diagnostic accuracy of the method. However, the major limitation of the cDTI is that this technique considers the diffusion of water molecules in the gray matter tissue as Gaussian, although it is hindered by interactions with other molecules and cell membranes (Jensen et al. 2005) and the gray matter is in fact largely isotropic (Pierpaoli and Basser 1996). This is why DTI parameters cannot provide reliable information on gray matter structural changes induced,

e.g., by α -synuclein deposition. Thus, DTI should be used mainly to detect the changes in white matter tracts which are more anisotropic. Information coming from the DTI parameters of the gray matter has been recently disputed and it has been suggested by some authors not to be taken into consideration (Zhuo et al. 2012).

In contrast to cDTI, diffusion kurtosis imaging (DKI), which is an extension of cDTI with more than 2 *b*-values used for data analysis, provides a feasible method to incorporate non-Gaussian water diffusion behavior in neural tissues (Jensen and Helpern 2010; Jensen et al. 2005). In order to quantify the degree of non-Gaussianity, metrics such as the mean, axial, and radial kurtosis (MK, AK, RK) are computed in addition to standard mean, axial, and radial diffusivity (MD, AD, RD) and FA metrics. This new diffusion kurtosis metrics are strongly associated with cellular microstructure, and therefore have higher potential than DTI to reveal useful information about neural tissue integrity in multiple diseases (Jensen and Helpern 2010; Jensen et al. 2005). Specifically, pre-clinical DKI studies with mice and rats revealed changes in the microstructural complexity of the brain in the mouse model of Alzheimer's disease (Vanhoutte et al. 2013), Huntington's disease (Blockx et al. 2012), traumatic brain injury model (Zhuo et al. 2012), chronic mild stress model of depression (Delgado y Palacios et al. 2011), experimental model of ischemia and stroke (Hui et al. 2012; Cheung et al. 2012) and in cuprizone-induced corpus callosum demyelination model (Falangola et al. 2014). In addition, DKI studies in PD patients have found significant changes of MK in the caudate nucleus, putamen, ipsilateral SN (Wang et al. 2011), and in the frontal, parietal, occipital, right temporal white matter, and lastly in anterior cingulate fiber as compared to those in the healthy controls (Kamagata et al. 2013, 2014); however, the direction of these changes remains controversial and the underlying pathological mechanisms for these changes are not well understood.

The aim of this study was to evaluate whether diffusion imaging as assessed by DKI metrics would provide a sensitive tool for differentiating between transgenic mice overexpressing human α -synuclein and wild-type (WT) littermates using (1) tract-based spatial statistics (TBSS), i.e., a voxel-based analysis which enables to identify changes in DKI parameters in the whole brain white matter without a prior hypothesis (a data-driven method) and (2) by performing the region of interest (ROI)-based analysis in brain structures that are known to show high α -synuclein accumulation. For the ROI analysis, conventional DTI (cDTI)-derived parametric maps (calculated from 2 *b*-values) were also computed in order to explore whether this widely used method can also capture microstructural

changes in our PD model. This transgenic model reproduces many features of sporadic PD, including progressive changes in dopamine release and striatal content, α -synuclein pathology, and early motor and non-motor deficits while it does not show major loss of neurons (Fleming et al. 2004, 2005; Chesselet 2008; Chesselet et al. 2012). This mouse model is particularly well suited to explore the early neuronal changes induced by α -synuclein accumulation (Chesselet et al. 2012).

Methods

Animals

Nine-month-old male transgenic mice overexpressing human wild-type α -synuclein under the murine Thy-1 promoter (TNWT-61) ($n = 7$) and WT ($n = 7$) were provided by QPS Austria (bred under license from UCSD). At the age of 9 months, animals develop clear PD-like symptomatology and there is robust presence of α -synuclein pathology in the brain (Chesselet et al. 2012). The animals were housed individually at the Central Animal Facility of Masaryk University, Brno, Czech Republic, maintained on a normal 12/12-h light/dark cycle, at constant relative humidity of 50–60 % and temperature of 22 ± 1 °C. Water and food were available ad libitum. All procedures were performed in accordance with EU Directive no. 2010/63/EU and approved by the Animal Care Committee of the Faculty of Medicine, Masaryk University, Czech Republic, in compliance with Czech Animal Protection Act No. 246/1992.

Behavioral Assessments

Challenging Beam Traversal Test, Pole test (Fleming et al. 2006; Schintu et al. 2009), Grid test (Sgado et al. 2011; Tillerson and Miller 2003), beam walk test (Suidan et al. 2013) were performed as described earlier in order to evaluate motor deficits.

Diffusion-Weighted MR Data Acquisition and Analysis

DKI data were obtained with a Bruker Avance 9.4T MRI system equipped with a gradient system with strength up to 660 mT/m. All experiments were performed using a quadrature volume coil (inner diameter 86 mm) for transmission and a 4-channel surface phased-array head coil as a receiver. Mice were anesthetized using isoflurane inhalation (1.5–2 %) and monitored to maintain constant physiological parameters. Fast low-angle shot (FLASH) scout images were used to localize the mouse brain. Reference

T2-weighted brain scans were acquired using 2D RARE (rapid acquisition with relaxation enhancement) sequence with the following acquisition parameters: 24 mm \times 24 mm field of view (FOV), 256 \times 256 acquisition matrix size, fifteen adjacent slices of 0.5-mm slice thickness. The echo-train length for each of the echoes was set to eight and the repetition time (TR) was 2500 ms with 4 averages for a total acquisition time of \sim 6 min. For the DKI acquisition, diffusion-weighted images were acquired with two-shot spin echo-echo planar imaging (SE-EPI). Respiratory gating was used to prevent motion artifacts. The generalized auto-calibrating partially parallel acquisitions (GRAPPA) with acceleration factor 2 were used to improve image quality and diminish susceptibility-caused artifacts. The DKI protocol included the acquisition of 6 b -values ($b = 0, 500, 1000, 1500, 2000, \text{ and } 2500 \text{ s/mm}^2$) and along 30 non-collinear directions, $\delta = 4$ ms, $\Delta = 11$ ms, 7 averages used for $b = 0$ acquisition and 4 averages for each other b -value. The SE-EPI sequence was recorded using the following parameters: FOV = 24 mm \times 24 mm, acquisition matrix = 98 \times 128, echo time TE = 25 ms using 300 kHz bandwidth, and TR \sim 5 s depending on respiratory rate, fifteen adjacent slices of 0.5 mm slice thickness, for a total acquisition time of approximately 1 h 40 min. The DKI data were processed and calculated on a voxel-by-voxel basis with 6 b -values to produce parametric maps (MD, AD, RD, FA, MK, AK, and RK), and also with 2 b -values to produce cDTI-derived parametric maps (MD, AD, RD and FA) in software called Explore DTI (Leemans et al. 2009). See Suppl. Fig. 1 for the data quality.

Tract-based Spatial Statistics (TBSS)

Further image analysis was carried out using tools of FSL (FMRIB Software Library, <http://www.fmrib.ox.ac.uk/fsl>) (Smith et al. 2004). Automatic brain extraction was carried out with BET on the same maps (Smith 2002), and then brain-extracted maps were checked one by one. Whole-brain voxel-based analysis of the white matter, tract-based spatial statistics (TBSS), was performed. TBSS (Smith et al. 2006) method was modified to fit it to the rodent brain (Sierra et al. 2011). All of the 3D FA volumes were registered together non-linearly, and using the registration matrices, the best registration target was chosen with a free-search method. The chosen study-specific volume was used as a template for the final transformations. Then the mean FA map was calculated and a skeleton was created at the threshold at FA = 0.2 representing the center of all tracts. Each mouse's aligned FA data was projected onto the skeleton. The process was done for all of the DKI maps. The general linear model design with permutation test (10,000 permutation) and cluster-based thresholding were

used with the predefined threshold ($t = 2.3$) to compare groups.

Region of Interest (ROI) Analysis

Averaged diffusion, FA, and kurtosis from both DKI and cDTI parametric maps were obtained from multiple regions: SN (1 slice), striatum (average of 5 slices), sensorimotor cortex (average of 5 slices), hippocampus (average of 3 slices), and thalamus (average of 2 slices). We choose these specific ROIs based on the substantial accumulation of α -synuclein found previously in 9-month old TNWT-61 mice (Chesselet et al. 2012). The ROIs on $b = 0$ images was drawn manually according to the Paxinos Mouse Brain Atlas (Paxinos and Franklin 2001) with the help of FA maps using ImageJ® software for the various brain regions as shown in the Suppl. Fig. 2.

Statistical Analysis

Both behavioral and MRI data were averaged using arithmetic mean and expressed as mean \pm SEM. A genotype effect (TNWT-61 vs. WT) was assessed for all behavioral tests and DKI/cDTI parameters using an unpaired two-tailed Student's t test or a Mann–Whitney U test if the dataset did not pass the Kolmogorov–Smirnov normality test. The level of statistical significance was set at $p < 0.05$. Additionally, we performed stepwise discriminant analysis using all parameters from the DKI protocol. We also performed the effect size analysis with ROI-based analysis in DKI and cDTI. Statistical analyses were performed using the software package Statistica 12 and SPSS20.

Results

Behavioral Study

We have evaluated the motor performance in TNWT-61 ($n = 7$) and WT ($n = 7$) mice and confirmed significant impairments in the TNWT-61 model. The transgenic mice made significantly more slips and needed more time to traverse the beam than the WT littermates in all beam tests—square beam: time ($p < 0.016$), number of slips ($p < 0.001$); round beam: time ($p < 0.001$), number of slips ($p < 0.001$); challenging beam traversal: time ($p < 0.007$), number of slips ($p < 0.001$). In the pole test, TNWT-61 mice showed worse performance only in turning behavior ($p < 0.001$); the time to descend the pole was not different from that of WT ($p = 0.8733$). Latency to fall in the grid test was significantly shorter in the TNWT-61

group as well ($p < 0.001$). The behavioral data are summarized in Fig. 1.

Diffusion-Weighted Imaging Study

TBSS Analysis

Increased kurtosis parameters were found in TNWT-61 mice compared to those in WT: (1) MK: bilaterally in the external capsule ($p = 0.007$); (2) AK: left-sided external capsule ($p = 0.029$); (3) RK: bilaterally in the external capsule, corpus callosum, cingulum, dorsal hippocampal commissure ($p = 0.003$) Decreased diffusivity parameters were found in TNWT-61 mice compared to those in WT: (1) MD: right mamillothalamic tract, right internal capsule, right nigrostriatal tract, right zona incerta ($p = 0.045$); (2) RD: bilaterally in the external capsule ($p = 0.018$). No other parameters showed differences between groups. The data are summarized in Fig. 2.

ROI analysis

As demonstrated in Fig. 3 TNWT-61 transgenic mice showed significant differences in DKI parameters as compared to the those in WT littermates. Specifically, the MK values were significantly elevated in the TNWT-61 group in almost all regions of interest except hippocampus: SN ($p = 0.03$, Cohen's $d = 1.824$), striatum ($p = 0.03$, Cohen's $d = 2.062$), sensorimotor cortex ($p = 0.05$, Cohen's $d = 1.523$), thalamus ($p = 0.003$, Cohen's $d = 2.544$). AK showed differences only in the striatum ($p = 0.03$, Cohen's $d = 1.940$) and thalamus ($p = 0.007$, Cohen's $d = 2.321$), while RK showed difference only in the thalamus ($p = 0.02$, Cohen's $d = 1.139$). We also found decrease in RD in the thalamus ($p = 0.02$, Cohen's $d = -1.979$).

With cDTI, we found decrease in MD, AD, and RD as compared to that in the WT littermates (Suppl. Fig. 3).

FA calculated from both DKI and cDTI protocols did not show any significant differences in the analyzed regions. Discriminant analysis showed that the MK in the thalamus was the most sensitive parameter to classify the data (81.8 % after cross-validation). No other parameter or combination of parameters reached a higher discriminant level.

Discussion

We confirmed the characteristic phenotype of strong motor coordination deficits in the TNWT-61 mice in the behavioral part of this study. This is in line with previous reports and provides evidence of dysfunction of the nigrostriatal

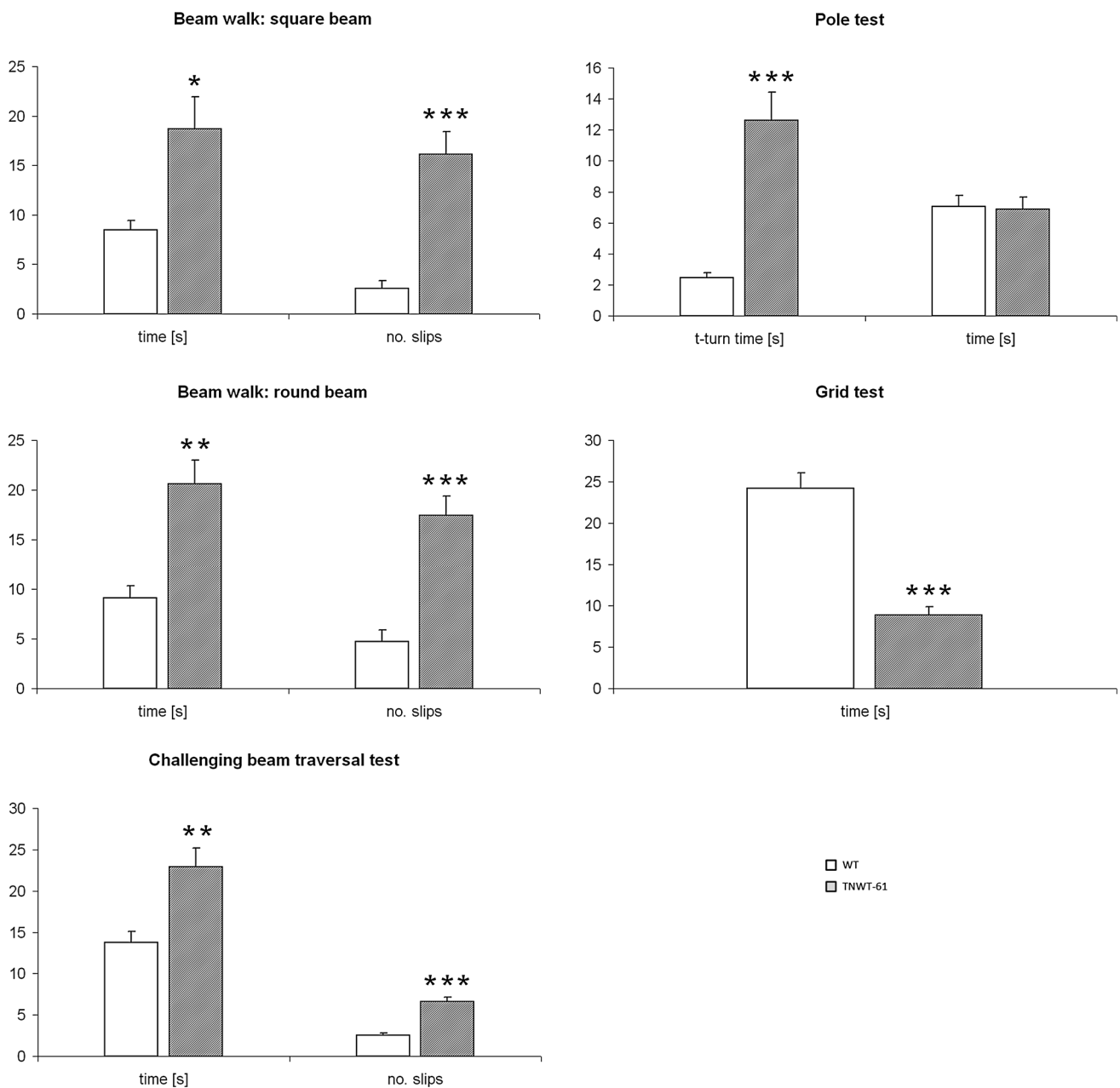


Fig. 1 The graphs represent behavioral motor impairments in TNWT-61 mice. Data are expressed as mean values \pm SEM, $n = 7$ for WT and $n = 7$ for TNWT-61, * $p < 0.05$, ** $p < 0.01$, *** $p < 0.001$

system. In the MRI part of the study, we assessed the potential of DKI to measure the microstructural changes induced by α -synuclein accumulation in white matter using for the first time TBSS analysis on mice DKI data. We also evaluated changes in gray matter using hypothesis-driven ROI method. Results from our study indicate that DKI can provide unique information in detecting the microstructural changes induced by α -synuclein in TNWT-61 mice that are complementary to and from the physiological point of view more reliable than the information obtained from cDTI. With the help of TBSS analysis, we found an increase in

kurtosis (MK, AK, and RK) and a decrease in diffusivity (MD and RD) parameters. The most affected regions were external capsule, mammillothalamic tract, dorsal hippocampal fissure, and zona incerta. Using the ROI-based analysis, we found an increase in kurtosis metrics in SN, striatum, sensorimotor cortex, and thalamus regions known to show α -synuclein accumulation in our PD model. Our findings thus accord with the results of Wang et al. (2011), and are in line with the hypothesis that the pathology induced by α -synuclein accumulation may result in microstructural changes that cause a decrease in free

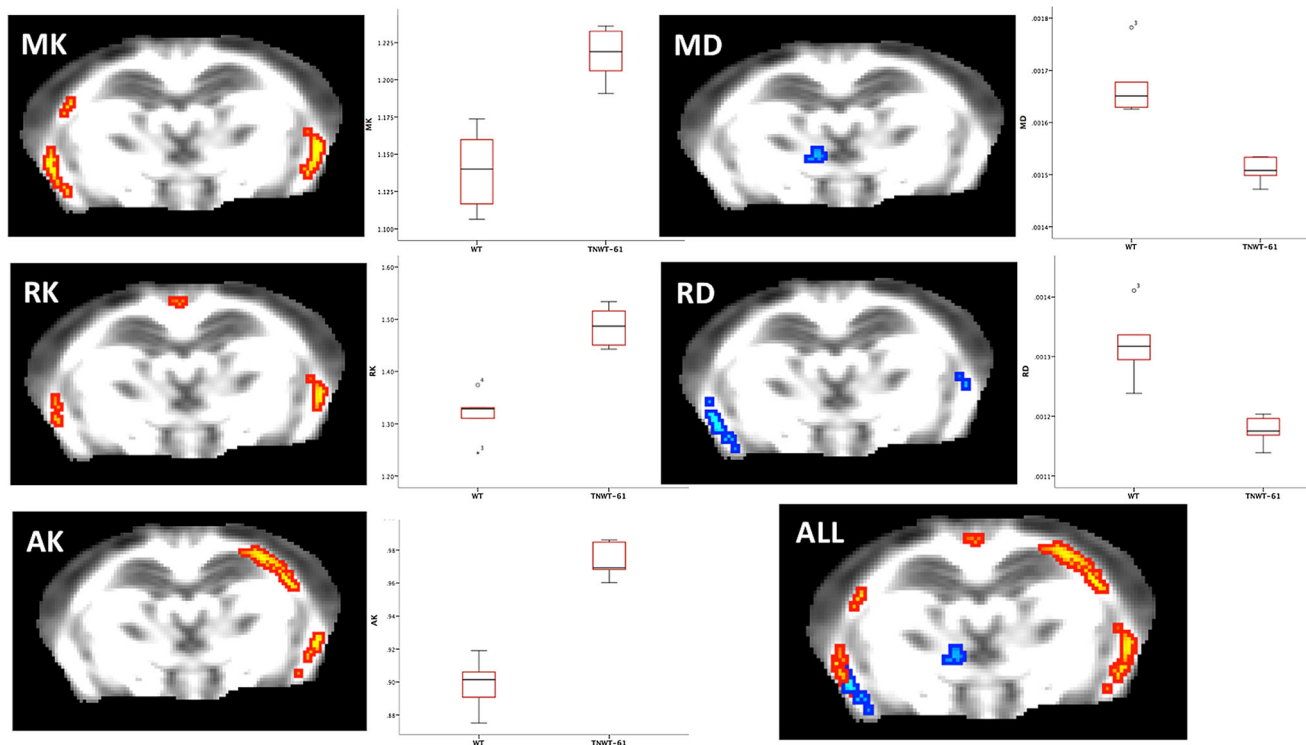


Fig. 2 TBSS: On the brain slices ($z = -2.5$ mm) marked regions show increased MK, RK, AK and decreased MD and RD. The sum of the results is presented in one single image as well (called ALL). Averaged diffusivity parameters under the affected regions are

represented with boxplots. Central mark on the boxplots is the mean, others present the 25 and 75 % percentiles and outliers are depicted black rings and stars

diffusion of water and hence are expressed by an increase in kurtosis metrics and decrease in diffusivity (Giannelli et al. 2012; Wang et al. 2011). Recently Delenclos et al. reported TNWT-61 overexpresses human α -synuclein in all the regions where we found the DKI changes. The DKI-derived kurtosis parameters were sensitive in detecting the abnormality in both white matter and gray matter. Interestingly, similar studies have been performed by Vanhoutte et al. with a transgenic mouse model of Alzheimer's disease (Vanhoutte et al. 2013). The authors found an increase in kurtosis due to accumulation of amyloid.

Recently, Kamagata et al. reported decrease in MK and FA in parietal, occipital, temporal white matter and cingulate fibers in PD patients (Kamagata et al. 2013, 2014). Unlike those authors, we have found an increase in MK in white matter in TNWT-61 mice. The reason for this discrepancy in direction of described changes might be due to the fact that our mice model is particularly characterized by overexpression of α -synuclein (Delenclos et al. 2014; Watson et al. 2012; Wang et al. 2011), while DKI as well as DTI changes described by Kamagata et al. in humans might be caused particularly by brain neurodegeneration (loss of neurons) and white matter tracts disruption (Kamagata et al. 2013; Schwarz et al. 2013).

It is necessary to point out that DKI was sensitive to depict microstructural changes in both white matter and gray matter in the transgenic model of PD but it may not be specific for the α -synuclein accumulation and could also reflect changes caused by other brain pathologies reported previously in this PD model, such as iron accumulation (Wang et al. 2011) or glial cell activation (Watson et al. 2012).

It is important to note that we also found a significant decrease in diffusivity parameters in our gray matter ROIs when the cDTI protocol was used (see Suppl. Fig. 3), while significant decrease in diffusivity was observed only in the thalamus when the DKI protocol was employed. This might be surprising but we would like to draw attention to the work of others (Jensen et al. 2005; Jensen and Helpert 2010) showing that estimation of DTI parameters from just $2b$ values (cDTI protocol) is not theoretically accurate and might lead to false-positive results.

Kurtosis is a unique, quite novel, and totally independent imaging metric. By assessing the non-Gaussian distribution of water, it reflects true water diffusion in the tissue and may thus be used as a complement to the cDTI dataset particularly for the detection of gray matter microstructural changes (see supplementary materials for the normalized diffusion-weighted decay in striatum of

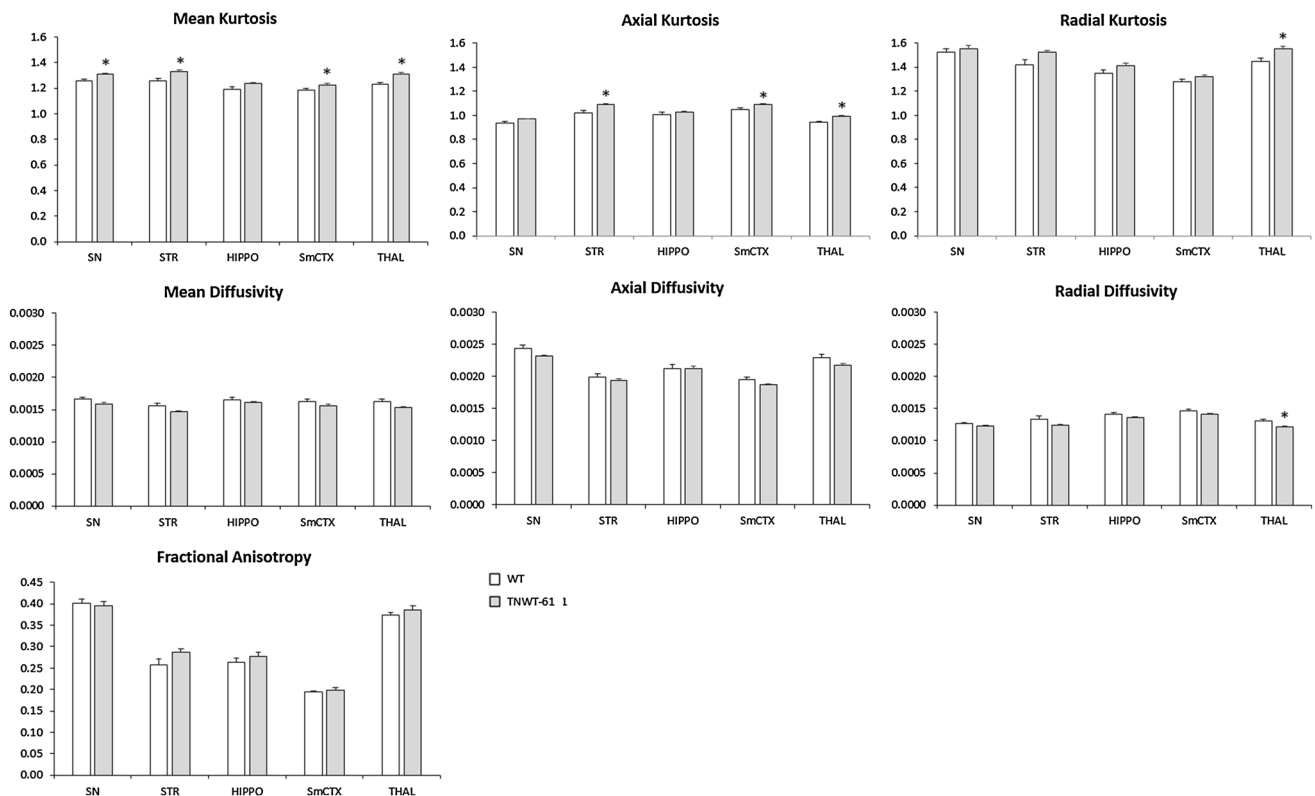


Fig. 3 ROI-based analysis: Bar graphs represent DKI parameters (WT wild-type mice, TNWT-61 transgenic mice, SN substantia nigra, STR striatum, HIPPO hippocampus, THAL thalamus, smCTX sensorimotor cortex). Kurtosis and fractional anisotropy are dimensionless

units; diffusivity values are given in mm^2/s . Data are expressed as mean values \pm SEM, $n = 5$ for WT and $n = 6$ for TNWT-61, * $p < 0.03$

both groups, Suppl. Fig. 4) (Steven et al. 2014). In order to assess the sensitivity of kurtosis and diffusivity parameters derived from the DKI protocol, we perform a step-by-step discriminant analysis and found that MK in the thalamus reached a discriminant level of almost 82 % for accurate classification of TNWT-61 from the WT group. No other parameter or combination of parameters reached a higher discriminant level.

Taken together, DKI provides additional information compared to cDTI in detecting alterations induced by α -synuclein accumulation in TNWT-61 mouse model of PD and hence it may improve the diagnosis of PD. Future studies should explore the exact underlying pathology for the kurtosis and diffusivity changes. Of note, the current study is part of an ongoing longitudinal study with planned DKI-pathological correlations. Further studies are also needed to shed light on potential usefulness of DKI as a biomarker for the pre-motor stages of PD.

Acknowledgments The transgenic mice were supplied for free by the QPS Austria GmbH, Grambach, Austria. The instruments for behavioral tests were kindly provided by Jiri Kucera, Environmental Measuring Systems, Brno, Czech Republic. The authors are grateful to Amy Chen and Heejae Chung for helping with English proof

reading. This work was supported by the project “Employment of Newly Graduated Doctors of Science for Scientific Excellence” (CZ.1.07/2.3.00/30.0009) co-financed from the European Social Fund and the state budget of the Czech Republic and by the project “CEITEC - Central European Institute of Technology” (CZ.1.05/1.1.00/02.0068) from the European Regional Development Fund. This study was also financed from the SoMoPro II programme. The research leading to this invention has acquired a financial grant from the People Programme (Marie Curie action) of the Seventh Framework Programme of EU according to the REA Grant Agreement No. 291782. The research is further co-financed by the South-Moravian Region. The study reflects only the author’s views and that the Union is not liable for any use that may be made of the information contained therein. The MR research was also supported by MEYS CR (LO1212), the MR unit and the animal facility (CZ62760225) infrastructure by MEYS CR and EC (CZ.1.05/2.1.00/01.0017) and by ASCR (RVO:68081731).

Compliance with Ethical Standards

Conflict of interest The authors declare no ethical or financial conflict of interest.

Human and Animal Rights and Informed Consent All procedures involving experimental animals were performed in accordance with EU Directive no. 2010/63/EU and approved by the Animal Care Committee of the Faculty of Medicine, Masaryk University, Czech Republic, in compliance with Czech Animal Protection Act No. 246/1992.

References

- Blockx I, Verhoye M, Van Audekerke J, Bergwerf I, Kane JX, Delgado YPR, Veraart J, Jeurissen B, Raber K, von Horsten S, Ponsaerts P, Sijbers J, Leergaard TB, Van der Linden A (2012) Identification and characterization of Huntington related pathology: an in vivo DKI imaging study. *NeuroImage* 63(2):653–662
- Boska MD, Hasan KM, Kibuule D, Banerjee R, McIntyre E, Nelson JA, Hahn T, Gendelman HE, Mosley RL (2007) Quantitative diffusion tensor imaging detects dopaminergic neuronal degeneration in a murine model of Parkinson's disease. *Neurobiol Dis* 26(3):590–596
- Chesselet MF (2008) In vivo alpha-synuclein overexpression in rodents: a useful model of Parkinson's disease? *Exp Neurol* 209(1):22–27
- Chesselet MF, Richter F, Zhu C, Magen I, Watson MB, Subramaniam SR (2012) A progressive mouse model of Parkinson's disease: the Thy1-aSyn ("Line 61") mice. *Neurotherapeutics* 9(2):297–314
- Cheung JS, Wang E, Lo EH, Sun PZ (2012) Stratification of heterogeneous diffusion MRI ischemic lesion with kurtosis imaging: evaluation of mean diffusion and kurtosis MRI mismatch in an animal model of transient focal ischemia. *Stroke* 43(8):2252–2254
- Cochrane CJ, Ebmeier KP (2013) Diffusion tensor imaging in parkinsonian syndromes: a systematic review and meta-analysis. *Neurology* 80(9):857–864
- Delenclos M, Carrascal L, Jensen K, Romero-Ramos M (2014) Immunolocalization of human alpha-synuclein in the Thy1-aSyn ("Line 61") transgenic mouse line. *Neuroscience* 277:647–664
- Delgado y Palacios R, Campo A, Henningsen K, Verhoye M, Poot D, Dijkstra J, Van Audekerke J, Benveniste H, Sijbers J, Wiborg O, Van der Linden A (2011) Magnetic resonance imaging and spectroscopy reveal differential hippocampal changes in anhedonic and resilient subtypes of the chronic mild stress rat model. *Biol Psychiatry* 70(5):449–457
- Falangola MF, Guilfoyle DN, Tabesh A, Hui ES, Nie X, Jensen JH, Gerum SV, Hu C, LaFrancois J, Collins HR, Helpem JA (2014) Histological correlation of diffusional kurtosis and white matter modeling metrics in cuprizone-induced corpus callosum demyelination. *NMR Biomed* 27(8):948–957
- Fleming SM, Salcedo J, Fernagut PO, Rockenstein E, Masliah E, Levine MS, Chesselet MF (2004) Early and progressive sensorimotor anomalies in mice overexpressing wild-type human alpha-synuclein. *J Neurosci* 24(42):9434–9440
- Fleming SM, Fernagut PO, Chesselet MF (2005) Genetic mouse models of parkinsonism: strengths and limitations. *NeuroRx* 2(3):495–503
- Fleming SM, Salcedo J, Hutson CB, Rockenstein E, Masliah E, Levine MS, Chesselet MF (2006) Behavioral effects of dopaminergic agonists in transgenic mice overexpressing human wildtype alpha-synuclein. *Neuroscience* 142(4):1245–1253
- Giannelli M, Toschi N, Passamonti L, Mascalchi M, Diciotti S, Tessa C (2012) Diffusion kurtosis and diffusion-tensor MR imaging in Parkinson disease. *Radiology* 265(2):645–646 **author reply 6-7**
- Hui ES, Du F, Huang S, Shen Q, Duong TQ (2012) Spatiotemporal dynamics of diffusional kurtosis, mean diffusivity and perfusion changes in experimental stroke. *Brain Res* 1451:100–109
- Jensen JH, Helpem JA (2010) MRI quantification of non-Gaussian water diffusion by kurtosis analysis. *NMR Biomed* 23(7):698–710
- Jensen JH, Helpem JA, Ramani A, Lu H, Kaczynski K (2005) Diffusional kurtosis imaging: the quantification of non-gaussian water diffusion by means of magnetic resonance imaging. *Magn Reson Med* 53(6):1432–1440
- Kamagata K, Tomiyama H, Motoi Y, Kano M, Abe O, Ito K, Shimoji K, Suzuki M, Hori M, Nakanishi A, Kuwatsuru R, Sasai K, Aoki S, Hattori N (2013) Diffusional kurtosis imaging of cingulate fibers in Parkinson disease: comparison with conventional diffusion tensor imaging. *Magn Reson Imaging* 31(9):1501–1506
- Kamagata K, Tomiyama H, Hatano T, Motoi Y, Abe O, Shimoji K, Kamiya K, Suzuki M, Hori M, Yoshida M, Hattori N, Aoki S (2014) A preliminary diffusional kurtosis imaging study of Parkinson disease: comparison with conventional diffusion tensor imaging. *Neuroradiology* 56(3):251–258
- Lang AE, Mikulis D (2009) A new sensitive imaging biomarker for Parkinson disease? *Neurology* 72(16):1374–1375
- Leemans A, Jeurissen B, Sijbers J, Jones DK (2009) ExploreDTI: a graphical toolbox for processing, analyzing, and visualizing diffusion MR data. In: 17th Annual Meeting of Intl Soc Mag Reson Med, Hawaii, USA
- Lerner A, Mogensen MA, Kim PE, Shiroishi MS, Hwang DH, Law M (2013) Clinical applications of diffusion tensor imaging. *World Neurosurg* 82(1–2):96–109
- Meijer FJ, Goraj B (2014) Brain MRI in Parkinson's disease. *Front Biosci (Elite edition)* 6:360–369
- Paxinos G, Franklin K (2001) The mouse brain in stereotaxic coordinates, 2nd edn. Academic Press, San Diego
- Pierpaoli C, Basser PJ (1996) Toward a quantitative assessment of diffusion anisotropy. *Magn Reson Med* 36(6):893–906
- Rascol O, Lozano A, Stern M, Poewe W (2011) Milestones in Parkinson's disease therapeutics. *Mov Disord* 26(6):1072–1082
- Rolheiser TM, Fulton HG, Good KP et al (2011) Diffusion tensor imaging and olfactory identification testing in early stage Parkinson's disease. *J Neurol* 258:1254–1260
- Schintu N, Frau L, Ibba M, Garau A, Carboni E, Carta AR (2009) Progressive dopaminergic degeneration in the chronic MPTP mouse model of Parkinson's disease. *Neurotox Res* 16(2):127–139
- Schwarz ST, Abaei M, Gontu V, Morgan PS, Bajaj N, Auer DP (2013) Diffusion tensor imaging of nigral degeneration in Parkinson's disease: a region-of-interest and voxel-based study at 3 T and systematic review with meta-analysis. *Neuroimage Clin* 3:481–488
- Sgado P, Viaggi C, Pinna A, Marrone C, Vaglini F, Pontis S, Mercuri NB, Morelli M, Corsini GU (2011) Behavioral, neurochemical, and electrophysiological changes in an early spontaneous mouse model of nigrostriatal degeneration. *Neurotox Res* 20(2):170–181
- Sierra A, Laitinen T, Lehtimäki K, Rieppo L, Pitkänen A, Gröhn O (2011) Diffusion tensor MRI with tract based spatial statistics and histology reveals undiscovered lesioned areas in kainate model of epilepsy in rat. *Brain Struct Funct* 216(2):123–135
- Smith SM (2002) Fast robust automated brain extraction. *Hum Brain Mapp* 17(3):143–155
- Smith SM, Jenkinson M, Woolrich MW, Beckmann CF, Behrens TE, Johansen-Berg H, Bannister PR, De Luca M, Drobnjak I, Flitney DE, Niazy RK, Saunders J, Vickers J, Zhang Y, De Stefano N, Brady JM, Matthews PM (2004) Advances in functional and structural MR image analysis and implementation as FSL. *Neuroimage* 23(Suppl 1):S208–S219
- Smith SM, Jenkinson M, Johansen-Berg H, Rueckert D, Nichols TE, Mackay CE, Watkins KE, Ciccarelli O, Cader MZ, Matthews PM, Behrens TE (2006) Tract-based spatial statistics: voxelwise analysis of multi-subject diffusion data. *Neuroimage* 31(4):1487–1505
- Soria G, Aguilar E, Tudela R, Mullol J, Planas AM, Marin C (2011) In vivo magnetic resonance imaging characterization of bilateral structural changes in experimental Parkinson's disease: a T2 relaxometry study combined with longitudinal diffusion tensor imaging and manganese-enhanced magnetic resonance imaging in the 6-hydroxydopamine rat model. *Eur J Neurosci* 33:1551–1560

- Steven AJ, Zhuo J, Melhem ER (2014) Diffusion kurtosis imaging: an emerging technique for evaluating the microstructural environment of the brain. *AJR Am J Roentgenol* 202(1):W26–W33
- Stocchi F, Olanow CW (2013) Obstacles to the development of a neuroprotective therapy for Parkinson's disease. *Mov Disord* 28(1):3–7
- Suidan GL, Duerschmied D, Dillon GM, Vanderhorst V, Hampton TG, Wong SL, Voorhees JR, Wagner DD (2013) Lack of tryptophan hydroxylase-1 in mice results in gait abnormalities. *PLoS One* 8(3):e59032
- Tillerson JL, Miller GW (2003) Grid performance test to measure behavioral impairment in the MPTP-treated-mouse model of parkinsonism. *J Neurosci Methods* 123(2):189–200
- Vaillancourt DE, Spraker MB, Prodoehl J et al (2009) High resolution diffusion tensor imaging in the substantia nigra of de novo Parkinson disease. *Neurology* 72:1378–1384
- Vanhoutte G, Pereson S, Delgado YPR, Guns PJ, Asselbergh B, Veraart J, Sijbers J, Verhoye M, Van Broeckhoven C, Van der Linden A (2013) Diffusion kurtosis imaging to detect amyloidosis in an APP/PS1 mouse model for Alzheimer's disease. *Magn Reson Med* 69(4):1115–1121
- Wang JJ, Lin WY, Lu CS, Weng YH, Ng SH, Wang CH, Liu HL, Hsieh RH, Wan YL, Wai YY (2011) Parkinson disease: diagnostic utility of diffusion kurtosis imaging. *Radiology* 261(1):210–217
- Watson MB, Richter F, Lee SK, Gabby L, Wu J, Masliah E, Effros RB, Chesselet MF (2012) Regionally-specific microglial activation in young mice over-expressing human wild type alpha-synuclein. *Exp Neurol* 237(2):318–334
- Zhuo J, Xu S, Proctor JL, Mullins RJ, Simon JZ, Fiskum G, Gullapalli RP (2012) Diffusion kurtosis as an in vivo imaging marker for reactive astrogliosis in traumatic brain injury. *NeuroImage* 59(1):467–477